The Role of Stellate Ganglion Induced Repolarization Heterogeneities in Post-Myocardial Infarction Arrhythmias: A Computational Approach

Lledo Nebot[1], Javier Villar-Valero[1], Juan F Gomez[2], Bastiaan JD Boukens[3,4], Beatriz Trenor[1]

[1]Centro de Investigación e Innovación en Bioingeniería, Universitat Politècnica de València, Valencia, Spain
[2]Valencian International University, Valencia, Spain
[3]Department of Experimental Cardiology, Leiden University Medical Center, Leiden, Netherlands
[4]Department of Physiology, University Maastricht, Maastricht University Medical Center, Maastricht, The Netherlands

Abstract

This study aimed to explore the influence of beta-adrenergic stimulation exerted by the stellate ganglia on the ventricles and its role in the generation of reentrant arrhythmias in post-myocardial infarction. It ultimately considered the potential of sympathetic denervation as a more specific alternative to cardioverter-defibrillators (ICDs) in antiarrhythmic therapy.

The digital twin of a patient who suffered a myocardial infarction with a scar in the posterior lateral region of the left ventricle was constructed based on cardiac magnetic resonance images with late gadolinium enhancement (LGE-CMR). The simulation included left stellate ganglion stimulation, increasing the slow delayed rectifier current (IKs) conductance, and thus reducing the action potential duration (APD). A finite element solver applied a clinical arrhythmia induction protocol based on a train of extra stimuli. Each case was simulated with and without APD changes in the innervated segments, replicating sympathetic stimulation. Results indicated that APD shortening due to sympathetic stimulation significantly increased the occurrence of reentrant arrhythmias, providing a deeper understanding of the mechanisms underlying ventricular tachycardia (VT).

1. Introduction

Cardiovascular diseases remain a significant cause of death worldwide, accounting for 32% of all reported deaths in 2019, as per the World Health Organization (WHO) [1], with 85% of those deaths resulting from heart attacks and strokes. The American Heart Association also reported that these diseases claimed 19.9 million lives worldwide in 2021 [2].

Following myocardial infarction, patients are at an elevated risk of death due to ventricular tachyarrhythmias, triggered by remodeling in the tissue surrounding the infarct, known as the infarct border zone (BZ). This BZ becomes a favorable substrate for the formation of reentry circuits and abnormal propagations due to alterations in the electrophysiological properties of the tissue, leading to possible changes in action potential duration (APD) [3]. Moreover, the presence of fibrosis plays a crucial role in the remodeling of the cardiac tissue, particularly impacting the excitability, conduction velocity, and overall electrical behavior of myocytes [4].

The stellate ganglion constitutes a set of nerves within the sympathetic trunk of the autonomic nervous system. Recent experimental studies [5] have demonstrated that in post-myocardial infarction patients, basal activity of the stellate ganglion increases, resulting in pro-arrhythmic effects. This increased activity initially causes a prolongation of the repolarization phase due to the activation of the L-type calcium current (ICaL), followed by a shortening of the repolarization phase caused by the slow delayed rectifier potassium current (IKs) [6]. This ultimately shortens the APD, potentially increasing the susceptibility of cardiac tissue to reentrant arrhythmias.

Thus, this study aims to investigate the effect of beta-adrenergic stimulation exerted by the stellate ganglia on the ventricles and its role in inducing reentrant arrhythmias post-myocardial infarction, using 3D patient-specific cardiac simulations. Additionally, we explored the potential of sympathetic denervation as an alternative and more targeted antiarrhythmic therapy compared to the use of cardioverter-defibrillators (ICDs).

2. Materials and Methods

2.1. Patient data

The data for this study were obtained from Teknon Medical Center in Barcelona, focusing on patients who had

experienced myocardial infarction and underwent an anatomical study of the affected area. Our selected patient had a scar located in the left lateral wall, a location particularly susceptible to the effects of sympathetic stimulation due to the influence of the left stellate ganglion. Moreover, this patient did experience ventricular tachycardia (VT) following the myocardial infarction, which has been experimentally recorded in the clinic.

2.2. Model and 3D simulations

Late gadolinium enhancement cardiac magnetic resonance imaging (LGE-CMR) was used to identify scar tissue and fibrosis in the infarcted left ventricular wall. The wall was segmented into 10 concentric layers, and color-coded pixel signal intensity (PSI) maps were projected onto these layers using trilinear interpolation. A PSI-based algorithm classified the hyperintense areas into core and BZ using thresholds of 40% ± 5% and 60% ± 5% of the maximum PSI, respectively [7]. From this, a 3D mesh of hexahedral elements with a 0.4 mm spatial resolution was created, and ventricular models were constructed, incorporating endocardial, mid-myocardial, and epicardial zones at 17%, 41%, and 42% of the wall thickness [8].

The reconstruction of the personalized model relied on the segmented LGE-CMR images. This process involved identifying and labeling the different cardiac structures, such as the right ventricle (RV), left ventricle (LV), septal regions, scar core, and BZ.

To model the infarcted heart, we used the ELVIRA simulation software [9], which implemented a modified version of the O'Hara et al. (2011) human ventricle cell model [10, 11], considering scar tissue as non-conductive, and adjusting BZ tissue to reflect post-infarction changes by reducing both longitudinal and transverse conductivities to 50% of the levels found in healthy tissue.

To simulate the presence of fibroblasts in the BZ a model based on MacCannell et al. (2007) [12] combined with the modified O'Hara myocyte model [10] was incorporated. This involved assigning fibroblast properties, such as reduced coupling with myocytes, — achieved by decreasing the diffusion coefficient by 50% [13]— to varying percentages of nodes in the BZ, with these properties distributed randomly using a probabilistic function.

2.3. Stimulation protocol

The BZ is a favorable substrate for arrhythmias, particularly when premature stimulation occurs within a critical vulnerable time window. To simulate these early stimuli, a protocol commonly used in clinical practice to induce ventricular tachycardia in vivo was applied. The protocol starts with the application of 6 baseline stimuli at a basic cycle length of 430 ms, followed by up to 3 additional early stimuli. These extra stimuli are introduced 300 ms after the last baseline or extra stimulus, with the interval progressively reduced in 10 ms intervals until the threshold for pulse propagation failure is identified. Subsequent extra stimuli are applied 20 ms after the last interval that allowed propagation. This process is repeated until the third extra stimulus is applied or until reentry is observed.

2.4. Stellate ganglion remodeling

As previously mentioned, the increase in stellate ganglion basal activity provokes an increase in the IKs current of healthy nodes in the areas affected by the left stellate ganglion, shown in Figure 1. Initially, to model this activity, various levels of IKs increases were tested, implementing a zero-dimensional (0D) model in MATLAB using the O'Hara model [9], to achieve the desired reduction in APD. It was found that multiplying the IKs current by a factor of 20 consistently results in a reduction of approximately 30% in APD [14]. After validating these findings, two patient-specific 3D cardiac models were created. One model included an increase in IKs, which resulted in a confirmed reduction in APD, representing stellate remodeling. The other model, without this remodeling, represented stellate denervation.

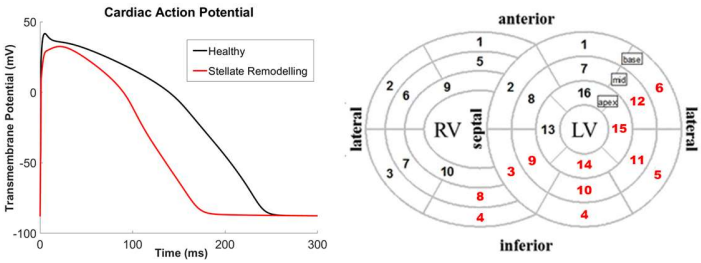

Figure 1. On the left, the a difference in APD between healthy nodes (in black) and those affected by the left stellate ganglion (in red). On the right, the affected American Heart Association (AHA) segments are depicted in red.

2.5. Recovery voltage interval (RVI)

To compare the effects of sympathetic stimulation, repolarization and activation maps are generated for both the remodeled and denervated heart models. These maps were created by elongating the sixth baseline pulse, providing insights into the heart's standard response to stimulation. Activation times refer to the time required for depolarization, while repolarization times indicate the total duration needed for the cardiac tissue to return to its resting state after depolarization.

Four maps were generated, two for the heart with stellate ganglion remodeling and two for the heart without

it. While activation maps are consistent in both scenarios, the differences observed in the repolarization maps reveal specific regions where repolarization times intersect with activation times. These intersections are crucial since they highlight areas at greater risk of arrhythmogenic activity.

The recovery voltage interval (RVI) was calculated using the method outlined in [15], where the RVI metric measures the likelihood of reentry by calculating the time between the wavefront reaching the exit site and nearby tissue becoming excitable again. Therefore, to calculate the RVI, the activation time at a BZ site is subtracted from the repolarization time at the healthy site. A negative RVI value indicates that the healthy tissue has been reactivated, suggesting a higher probability of reentry.

For the calculation of RVI, we selected four regions: two where reentry was induced in both simulations and two chosen visually from the maps based on regions with lower repolarization times compared to activation times. In each case, the healthy node with the lowest repolarization value in the area was identified, and an 8 mm sphere was defined around this node. RVI was then computed using the repolarization time of the central node and the activation times of adjacent BZ nodes within the sphere. The average RVI values were calculated, with the minimum value confirming the area's most prone to reentry.

3. Results

The stimulation protocol previously described was applied to the two patient-specific cardiac models, one with stellate remodeling and the other with stellate denervation. Reentry patterns were examined in both conditions, with reentry being triggered by the third extra stimulus in each case, as illustrated in Figures 2 and 3. Specifically, with denervation, reentry was observed at 270 ms after the second extra stimulus, whereas with stellate remodeling, it occurred at 260 ms after the second extra stimulus.

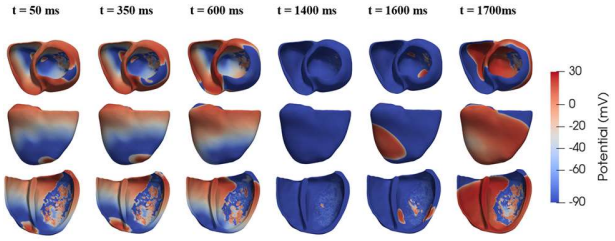

Figure 2. Time evolution of the reentry scenario with stellate ganglion denervation applied.

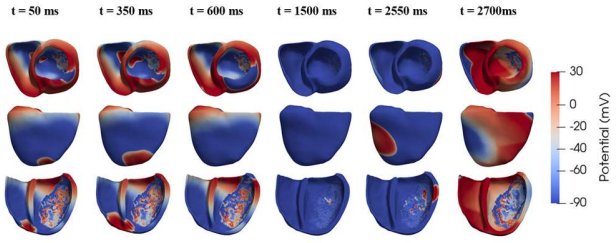

Figure 3. Time evolution of the reentry scenario with stellate ganglion remodeling applied.

Based on the activation and repolarization maps described previously, regions with significant variations in RVI were identified. While ideally RVI would be calculated for all nodes in the cardiac model to generate a comprehensive map, this study focused on regions with observable reentry (sites 1 and 3) and additional areas with distinct repolarization differences between remodeled and denervated conditions (sites 2 and 4). These four sites are illustrated in Figure 4, with detailed RVI calculations presented in Table 1.

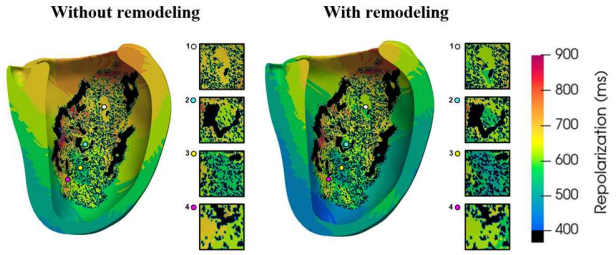

Figure 4. Details of sites selected for RVI calculation.

Only site 3 in the denervated model exhibited a negative RVI value in both its mean and minimum measurements, indicating that this site was the only region showing a higher risk of reentry in these conditions. In contrast, when examining the stellate remodeled model, all selected sites showed negative RVI values, significantly increasing the number of regions susceptible to reentry compared to those observed in the denervated model.

Table 1. RVI Calculation in the four sites depicted in Figure 4 (ms)

	Stellate denervation		**Stellate remodeling**	
Site	Mean	Minimum	Mean	Minimum
1	422	240	-275	-460
2	364	10	-102	-460
3	-12	-270	-90	-350
4	410	110	-98	-400

4. Discussion and conclusion

The study's results show that stellate ganglion remodeling significantly increases the susceptibility of cardiac tissue to reentrant arrhythmias, with remodeled conditions leading to an increased number of regions exhibiting negative RVI values, indicating a higher risk for reentry. This increase in reentry-prone areas deviates from the denervated conditions, where only one site demonstrated this tendency, emphasizing the critical role that stellate ganglion remodeling plays in arrhythmogenesis, specifically by altering the electrophysiological properties of the BZ tissue post-myocardial infarction.

Furthermore, the study could validate the use of RVI and the generation of repolarization and activation maps as reliable measures for identifying and monitoring arrhythmogenic zones. The consistent results of negative RVI values in remodeled conditions, when compared to those in denervated models, reinforce the utility of RVI in evaluating the likelihood of reentrant activity. This is critical for both clinical diagnosis and the strategic planning of therapeutic interventions.

The data also suggest that sympathetic denervation could be a promising alternative to conventional treatments such as cardioverter-defibrillators (ICDs) for managing arrhythmias. By reducing the sympathetic influence on cardiac tissue, denervation could potentially lower the risk of arrhythmias by minimizing the development of reentry-prone zones.

In conclusion, the study emphasizes the significant impact of stellate ganglion remodeling on arrhythmic risk. This suggests that sympathetic denervation could be a valuable alternative to ICDs for managing arrhythmias. Additionally, combining repolarization and activation maps alongside RVI calculations might enhance the precision of arrhythmia risk assessment by improving the identification of high-risk areas.

Acknowledgments

This work was supported by Grant PRE2020-091849 [MCIN/AEI/10.13039/501100011033] and “ESF Investing in your future”; Grant PID2019-104356RB-C41 [MCIN/AEI/10.13039/501100011033]; PID2022-136273OA-C33 and PID2022-140553OB- C41 [MICIU/AEI/10.13039/501100011033 and by ERDF/EU]; Barcelona Supercomputing Center [IM-2021-1-0001 and IM-2021-3 0001] and in MareNostrum5 (IM-2024-1-0010 and IM-2024-2-0015).

Oracle Cloud credits and related resources by Oracle for Research.

References

[1] Cardiovascular diseases (CVDs). World Health Organization 2021. Available at: https://www.who.int/news-room/fact-sheets/detail/cardiovascular-diseases-(cvds) (accessed July 29, 2024).

[2] S. S. Martin et al. “2024 Heart Disease and Stroke Statistics: A Report of US and Global Data From the American Heart Association,” *Circ*., vol. 149, no. 8, Feb. 2024.

[3] P. Colli-Franzone, et al. “Role of Infarct Scar Dimensions, Border Zone Repolarization Properties and Anisotropy in the Origin and Maintenance of Cardiac Reentry,” *Math. Biosci.*, vol. 315, pp. 108228, Sep. 2019.

[4] C. M. Costa, et al. “Modeling the Electrophysiological Properties of the Infarct Border Zone,” *Front. in Psych*., vol. 9, pp. 338147, Apr. 2018.

[5] S. Han et al. “Electroanatomic Remodeling of the Left Stellate Ganglion After Myocardial Infarction,” *Jour. of the Amer. Coll. of Card.*, vol. 59, no. 10, pp. 954-961, Mar. 2012.

[6] V. M. Meijborg et al. “Stellate ganglion stimulation causes spatiotemporal changes in ventricular repolarization in pig,” *Heart Rhyt.*, vol. 17, no. 5, pp. 795-803, May 2020.

[7] B. Jáuregui et al. "Cardiovascular magnetic resonance determinants of ventricular arrhythmic events after myocardial infarction," *Europace*, vol. 24, no. 6, pp. 938-947, July 2022.

[8] A. Lopez-Perez et al. "Personalized Cardiac Computational Models: From Clinical Data to Simulation of Infarct-Related Ventricular Tachycardia," *Front. in Phys*., vol. 10, May 2019.

[9] E. A. Heidenreich, et al. "Adaptive macro finite elements for the numerical solution of monodomain equations in cardiac electrophysiology," *Ann. Biomed Eng.,* vol. 38, no. 7, pp. 2331-2345, July 2010.

[10] T. O'Hara, L. Virág, , A. Varró and Y. Rudy, “Simulation of the Undiseased Human Cardiac Ventricular Action Potential: Model Formulation and Experimental Validation,” *PLoS Comp. Biol.,* vol. 7, no. 5, May 2011.

[11] S. Dutta, et al. “Electrophysiological properties of computational human ventricular cell action potential models under acute ischemic conditions,” *Prog. Bioph. Mol. Biol*., vol. 129, pp. 40-52, Feb 2017.

[12] K. MacCannell et al. “A Mathematical Model of Electrotonic Interactions between Ventricular Myocytes and Fibroblasts”. *Biophy. Jour*., vol. 92, no. 11, pp. 4121-4132, Feb 2007.

[13] J. Gomez, K. Cardona, L. Romero, J. Ferrero and B. Trenor, “Electrophysiological and Structural Remodeling in Heart Failure Modulate Arrhythmogenesis. 1D Simulation Study,” *PLoS One*, vol. 9, no. 9, e106602, Sep 2014.

[14] B. J. D. Bastiaan et al. “Mechanism of ventricular premature beats elicited by left stellate ganglion stimulation during acute ischaemia of the anterior left ventricle," Card. res. vol. 117, no. 9, pp. 2083-2091, Aug. 2020.

[15] F. O. Campos et al. “Characterizing the clinical implementation of a novel activation-repolarization metric to identify targets for catheter ablation of ventricular tachycardias using computational models,” *Comp. Biol. Med.,* vol. 108, pp. 263-275, May 2019.

Address for correspondence:

Beatriz Trenor
Centro de Investigación e innovación en Bioingenieria (Ci2B),
Universitat Politècnica de València (UPV)
Camino de Vera s/n, 46022 Valencia, Spain
Email: btrenor@eln.upv.es